Extent of the Ross Orogen in Antarctica: new data from DSDP 270 and Iselin Bank

N. MORTIMER[1], J.M. PALIN[2], W.J. DUNLAP[3] and F. HAUFF[4]

[1]*GNS Science, Private Bag 1930, Dunedin, New Zealand*
[2]*Department of Geology, University of Otago, PO Box 56, Dunedin, New Zealand*
[3]*Department of Geology and Geophysics, University of Minnesota, Minneapolis MN 55455, USA*
[4]*IFM-GEOMAR Leibniz Institute for Marine Sciences, Wischhofstrasse 1–3, D-24148 Kiel, Germany*
n.mortimer@gns.cri.nz

Abstract: The Ross Sea is bordered by the Late Precambrian–Cambrian Ross–Delamerian Orogen of East Antarctica and the more Pacific-ward Ordovician–Silurian Lachlan–Tuhua–Robertson Bay–Swanson Orogen. A calcsilicate gneiss from Deep Sea Drilling Project 270 drill hole in the central Ross Sea, Antarctica, gives a U-Pb titanite age of 437 ± 6 Ma (2σ). This age of high-grade metamorphism is too young for typical Ross Orogen. Based on this age, and on lithology, we propose a provisional correlation with the Early Palaeozoic Lachlan–Tuhua–Robertson Bay–Swanson Orogen, and possibly the Bowers Terrane of northern Victoria Land. A metamorphosed porphyritic rhyolite dredged from the Iselin Bank, northern Ross Sea, gives a U-Pb zircon age of 545 ± 32 Ma (2σ). The U-Pb age, petrochemistry, Ar-Ar K-feldspar dating, and Sr and Nd isotopic ratios indicate a correlation with Late Proterozoic–Cambrian igneous protoliths of the Ross Orogen. If the Iselin Bank rhyolite is not ice-rafted debris, then it represents a further intriguing occurrence of Ross basement found outside the main Ross–Delamerian Orogen.

Introduction

The Ross Sea lies between East and West Antarctica (Fig. 1). Most of the East Antarctica-Ross Sea margin is bordered by rocks of the Ross Orogen (Stump 1995), which comprise Late Proterozoic siliciclastic, carbonate and minor igneous protoliths (Wilson Terrane and Skelton Group; Laird 1991, Cook & Craw 2002 and references therein). These rocks underwent deformation, greenschist to (mainly) amphibolite facies metamorphism and intrusion by granitoid plutons in the Cambrian. Similar rocks are found along strike in the Delamerian Orogen of Australia with which the Ross Orogen was formerly continuous (Fig. 1). In contrast, the West Antarctica-Ross Sea margin is bordered by a younger orogen comprising protoliths of comparatively monotonous greenschist facies Ordovician siliciclastic rocks (Swanson Formation), that were intruded by granitoids of Devonian–Carboniferous age. These West Antarctic rocks are similar to rocks of the Robertson Bay Terrane in northern Victoria Land, Buller Terrane of New Zealand and Lachlan Orogen of Australia in that they are all arguably part of the same Early Palaeozoic Gondwana orogenic belt with protoliths, deformation and metamorphism largely younger than the rocks of the Ross Orogen (Wade & Couch 1982, Laird 1991, Bradshaw 2007, Bradshaw *et al.* 2009). Figure 1 shows this interpretation. Between the Ross–Delamerian orogens, and also occurring as fault bounded slices within each, are Cambrian boninitic-basaltic rocks with clastic and minor carbonate elements (e.g. Bowers Terrane & Takaka Terrane, Fig. 1). Collectively, all the aforementioned tectonic elements are part of the wider Terra Australis Orogen of Cawood (2005). The youngest and most Pacific-ward orogen in Fig. 1, which is not the subject of this paper, is the Mesozoic Amundsen–Median Batholith–Rangitata Orogen.

A topic of ongoing interest in the Ross Sea region is to track the interpolated and extrapolated extent of the aforementioned orogenic belts between West Antarctica, East Antarctica, Australia and Zealandia. When present-day onland outcrops are restored on a Gondwanaland continental reconstruction (Fig. 1) they are still separated by distances of up to thousands of kilometres. The purpose of this short paper is to report the results of geochronological, petrochemical and tracer isotopic data from two remote offshore localities in the Ross Sea: 1) Deep Sea Drilling Project (DSDP) site 270, and 2) Iselin Bank, and to discuss with which orogenic belts samples from these features correlate.

Analytical methods are given in the table captions. Complete sample data have also been lodged in the PETLAB database (http://pet.gns.cri.nz, see P50869 and P78670).

DSDP 270

DSDP 270 was drilled in the central Ross Sea (77.441°S, 178.503°W) in 1973. After penetrating 413 m of Cenozoic
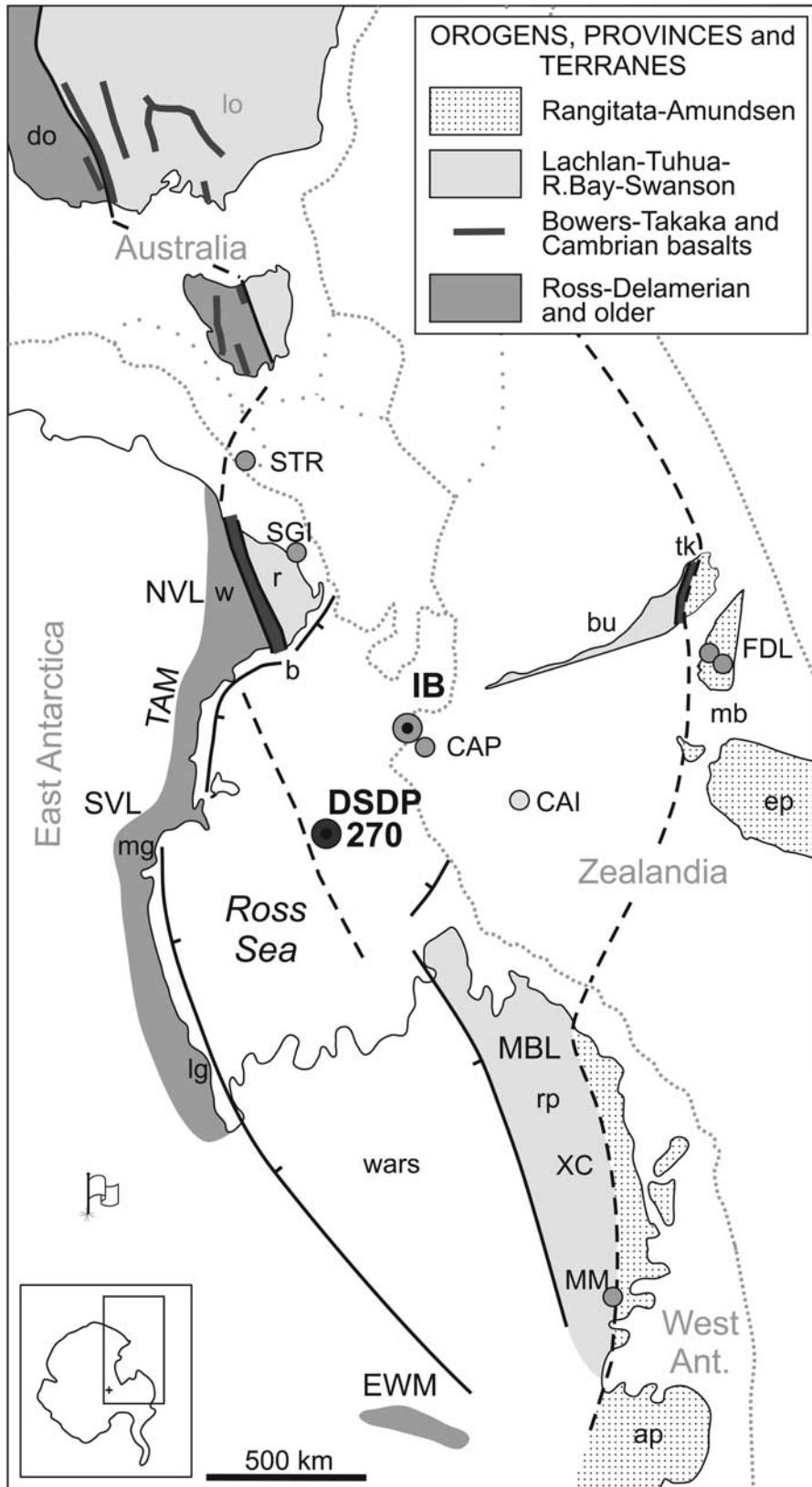
Fig. 1. Location map of the two sample sites: DSDP 270 and RV *S.P. Lee* dredge site 17 on the edge of the Iselin Bank. East and West Antarctica are shown in present-day co-ordinates with Zealandia and Australian restored to their approximate pre-Gondwana breakup locations. Palaeogeography and geology are adapted from Challis *et al.* (1982), Pankhurst *et al.* (1998), Fioretti *et al.* (2005a, 2005b), Glen (2005), Adams (2007) and Bradshaw (2007). Geographic features and sample sites: STR = South Tasman Rise, SGI = Surgeon Island, TAM = Transantarctic Mountains, NVL = northern Victoria Land, SVL = southern Victoria Land, IB = Iselin Bank, CAP = Campbell Plateau, CAI = Campbell Island, FDL = Fiordland, MBL = Marie Byrd Land, XC = Executive Committee Range, MM = Mount Murphy, EWM = Ellsworth Mountains. Geological units: do = Delamerian Orogen, lo = Lachlan Orogen, w = Wilson Terrane, b = Bowers Terrane, r = Robertson Bay Terrane, bu = Buller Terrane, tk = Takaka Terrane, mb = Median Batholith, ep = Eastern Province, wars = West Antarctic Rift System, mg = Mulock Granite, lg = Liv Group, rp = Ross province (Pankhurst *et al.* 1998; not to be confused with Ross Orogen), ap = Amundsen province.
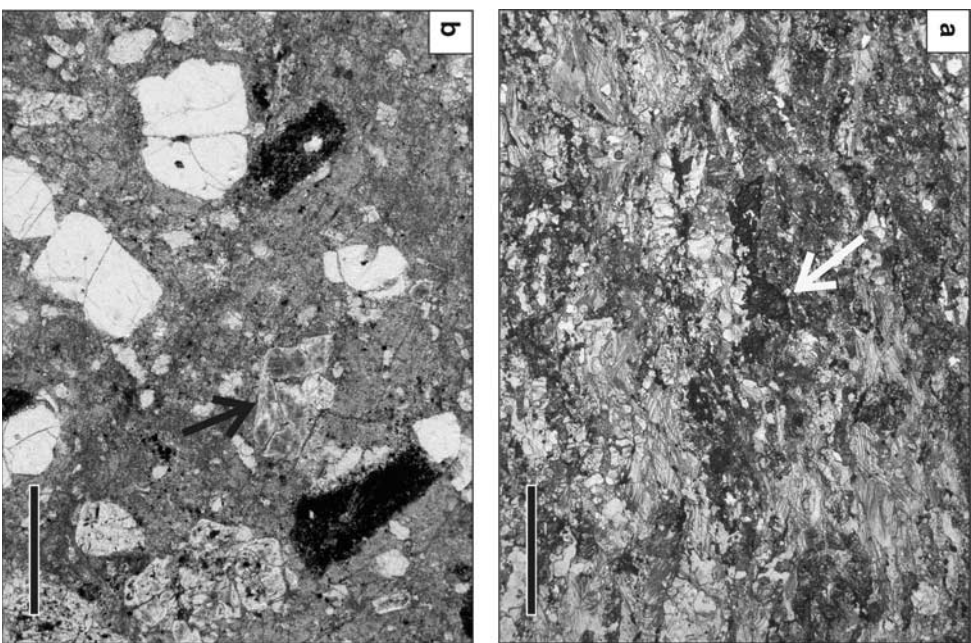
Fig. 2. Thin section images of **a.** P78670, calcsilicate gneiss from DSDP 270 with feldspar (pale), calcite (dark grey) and titanite (arrowed), and **b.** P50869, metarhyolite from Iselin Bank, with phenocrysts of quartz (white), K-feldspar (arrowed), plagioclase (mottled, right hand side) and altered biotite (black). Both images plane polarized light, scale bar = 1 mm.

sedimentary rocks, it bottomed in 10m of calcsilicate gneiss and marble, 25% of which was recovered. In their initial report, Ford & Barrett (1975) correlated DSDP 270 basement with the Skelton Group of the Ross Orogen. Subsequently, Fitzgerald & Baldwin (1997) reported a mean fission track age of 103 ± 22 Ma (2σ) from 16 apatite grains. So far as we are aware, there has been no other analytical work done on the basement material from DSDP 270.

We obtained a piece of calcsilicate gneiss from the International Ocean Drilling Programme repository with the sample designation Leg 28, Site 270, Core 49R, Section 01W, Interval 125–132 cm. This was given the GNS Science (Institute of Geological and Nuclear Sciences) sample number P78670 and a thin section and mineral separate were made. We can add little to the petrographic description given by Ford & Barrett (1975). In summary the

Table I. U-Th-Pb isotope data for ten titanite grains from sample P78670, DSDP 270 calcsilicate gneiss.

Spot no.	Pb* (ppm)	U (ppm)	Atomic Th/U	Measured isotope ratios and 1σ (%) internal errors				Common-Pb corrected ages and 1σ absolute internal errors (Ma)			6*/38-7*/35 agreement (%)	% Common ^{206}Pb	Spot MSWD	Selected common-Pb correlated age and 1σ absolute external error (Ma)
				^{206}Pb/^{238}U	^{207}Pb/^{235}U	^{207}Pb/^{206}Pb	^{208}Pb/^{232}Th	^{206}Pb*/^{238}U	^{207}Pb*/^{235}U	^{207}Pb*/^{206}Pb*				
01	9.31	106	1.01	0.07274 ± 0.7	0.8460 ± 2.3	0.0844 ± 2.2	0.02691 ± 1.3	438.4 ± 3.5	449.3 ± 22.7	505.1 ± 24.7	99	3.3	2.90	438.4 8.2
02	7.00	64	0.58	0.09341 ± 0.8	3.0927 ± 1.6	0.2401 ± 1.4	0.10954 ± 3.0	445.1 ± 4.1	351.4 ± 49.1	rd	129	23.5	2.83	445.1 8.6
03-r	29.65	366	0.56	0.07372 ± 0.6	0.8587 ± 1.4	0.0845 ± 1.3	0.03425 ± 1.1	438.9 ± 2.4	385.1 ± 13.5	74.6 ± 3.0	115	4.4	2.78	438.9 7.8
03-c	29.70	289	0.57	0.09029 ± 0.8	1.9438 ± 2.4	0.1561 ± 2.2	0.06955 ± 1.6	485.3 ± 4.1	384.5 ± 38.6	rd	128	13.4	3.03	rd
04	7.61	94	0.26	0.07840 ± 0.7	1.2006 ± 1.8	0.1111 ± 1.6	0.06769 ± 1.2	453.1 ± 3.3	424.5 ± 17.0	272.2 ± 11.6	107	7.1	2.23	453.1 8.3
05	9.49	113	0.27	0.07969 ± 0.8	1.4672 ± 2.1	0.1335 ± 1.9	0.08349 ± 1.7	446.7 ± 3.6	410.6 ± 23.5	212.7 ± 13.3	110	9.9	2.34	446.7 8.4
06	17.83	237	0.27	0.07329 ± 0.6	0.9373 ± 1.3	0.0928 ± 1.1	0.04891 ± 1.2	434.8 ± 2.4	418.0 ± 10.2	326.5 ± 8.2	105	4.8	3.01	434.8 7.7
07	11.80	115	1.73	0.07333 ± 0.7	0.9913 ± 3.1	0.0981 ± 3.0	0.02712 ± 1.2	427.2 ± 3.5	345.5 ± 39.5	rd	126	6.6	1.54	427.2 8.1
08	9.05	124	0.31	0.07129 ± 0.6	0.7553 ± 2.6	0.0768 ± 2.5	0.03665 ± 1.8	430.7 ± 2.8	403.6 ± 14.9	251.1 ± 9.9	107	3.1	1.52	430.7 7.7
09	7.68	89	0.25	0.08035 ± 1.0	1.8795 ± 3.6	0.1697 ± 3.5	0.11910 ± 4.1	428.2 ± 5.4	382.0 ± 66.6	111.5 ± 22.0	113	14.5	1.68	428.2 9.1
10	11.60	163	0.15	0.07181 ± 0.5	0.8879 ± 2.3	0.0897 ± 2.3	0.06482 ± 2.2	427.8 ± 2.3	410.1 ± 16.6	312.3 ± 13.1	105	4.5	1.50	427.8 7.5
weighted mean of selected common-Pb corrected ages (n = 10 of 11, MSWD = 1.2, 1σ absolute external error)														437 3

Analyses perfomed at Australian National University using a pulsed LambdaPhysik LPX 120I UV ArF excimer laser. Analytical methods described by Scott *et al.* (2009) and references therein. All errors are 1σ, * = radiogenic component only, d = discordant, rd = reversely discordant, r = rim, c = core. Spot-MSWD calculated on basis of scatter of observed data with increasing depth during individual spot measurement.
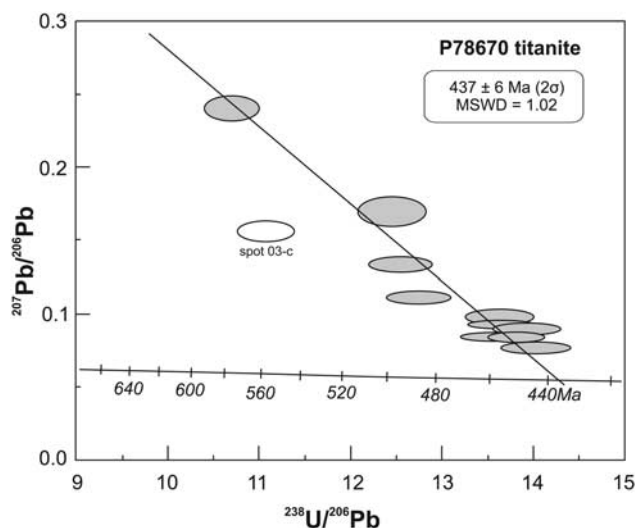
Fig. 3. Tera-Wasserburg plot of uncorrected U-Pb analyses of titanite from P78670. Intercept line is projected from common Pb at $^{207}Pb/^{206}Pb = 0.81 \pm 0.05$.

main minerals (in descending order of abundance) are calcite, quartz, chlorite (probably after biotite), feldspar, clinozoisite, titanite and diopside (Fig. 2a). The rock shows a gneissic texture and is visibly altered and retrograded. The heavy fractions of the mineral separate contained no zircon, but yielded good, large titanite grains.

U-Pb titanite data

Ten grains of titanite from P78670 were analysed for U-Th-Pb isotopes by LA-ICP-MS (Table I). The data for all grains are discordant on a Tera-Wasserburg plot (Fig. 3) and one core analysis, spot 03-c, fell away from the rest of the group. A number of different ways of calculating a U-Pb titanite age give essentially the same result. The weighted mean of ten out of eleven analyses is 437 ± 6 Ma (2σ), the same as the lower intercept age of ten out of eleven analyses projected from common Pb. Linear regression of all 11 analyses, not projected from a common Pb point, is 432 ± 18 Ma (2σ). Thus the estimated age is not sensitive to the choice of common Pb isotopic composition and no resolvable age variation within grains is indicated by the scatter of the observed data. We interpret calcsilicate gneiss P78670 to record an age of amphibolite facies metamorphism of 437 ± 6 Ma (early Silurian).

Iselin Bank

The Iselin Bank lies at the edge of the Ross Sea continental shelf at water depths < 2000 m (Fig. 1). In 1984, during cruise L2-84-AN of the RV *S.P. Lee*, rocks were dredged from two locations on the Iselin Bank (Wong *et al.* 1987). The dredges were dominated by glacially-transported

Table II. Whole rock geochemical and isotopic data for P50869 meta-rhyolite.

SiO_2 (XRF wt%)	75.83
TiO_2	0.16
Al_2O_3	12.81
Fe_2O_3T	1.75
MnO	< 0.01
MgO	0.21
CaO	0.42
Na_2O	2.47
K_2O	4.68
P_2O_5	0.03
LOl	1.32
Total	99.66
Ba (ICP-MS ppm)	359
Ce	92.9
Co	71.1
Cr	1.23
Cs	6.32
Cu	1.97
Dy	8.02
Er	4.30
Eu	0.35
Ga	19.1
Gd	8.61
Hf	3.80
Ho	1.55
La	43.7
Li	12.8
Mo	0.169
Nb	5.98
Nd	41.3
Ni	0.842
Pb	27.3
Pr	11.3
Rb	233
Sb	0.315
Sc	4.88
Sm	8.68
Sn	9.87
Sr	58.1
Ta	0.574
Tb	1.33
Th	21.0
Tl	1.24
Tm	0.633
U	3.95
V	3.82
Y	45.4
Yb	4.12
Zn	52.8
Zr	103
$^{87}Sr/^{86}Sr$ (TIMS)	0.791007 ± 5
$^{143}Nd/^{144}Nd$	0.511987 ± 2
$^{206}Pb/^{204}Pb$	18.418 ± 1
$^{207}Pb/^{204}Pb$	15.636 ± 1
$^{208}Pb/^{204}Pb$	38.123 ± 1
$^{87}Sr/^{86}Sr$ @ 545Ma	0.700129
εNd @ 545Ma	-7.9

Methods: XRF = X-ray fluorescence (Kennedy *et al.* 1983), ICP-MS = inductively coupled plasma mass spectrometry (Garbe-Schönberg 1993), TIMS = thermal ionization mass spectrometry (Hoernle *et al.* 2004).

debris, but one rhyolitic sample, sample 17-3b-10, had a freshly broken surface and was the only rock thought to be possibly *in situ*. The dredge-on-bottom co-ordinates of RV

Table III. U-Th-Pb isotope data for eight zircons from sample P50869, Iselin Bank meta-rhyolite.

Spot no.	Pb* (ppm)	U (ppm)	Atomic Th/U	Measured isotope ratios and 1σ (%) internal errors				Common-Pb corrected ages and 1σ absolute internal errors (Ma)			6*/38-7*/35 agreement (%)	% common 206Pb	Spot MSWD	Selected common-Pb correlated age and 1σ absolute external error (Ma)
				206Pb/238U	207Pb/235U	207Pb/206Pb	208Pb/232Th	206Pb*/238U	207Pb/235U	207Pb*/206Pb*				
7	147.0	5540	0.47	0.02459 ± 1.9	0.2761 ± 2.2	0.0814 ± 1.3	0.01303 ± 2.5	148.6 ± 2.8	118.3 ± 6.7	rd	126	5.2	81	rd
2	200.5	3960	0.63	0.04440 ± 2.0	0.6236 ± 3.5	0.1019 ± 2.9	0.02564 ± 3.5	255.3 ± 5.3	134.3 ± 28.3	rd	190	9.0	205	rd
4	125.1	2329	0.48	0.04956 ± 1.6	0.6431 ± 4.2	0.0941 ± 3.8	0.02679 ± 3.4	295.1 ± 4.9	277.5 ± 29.2	132.2 ± 14.7	106	5.5	104	d
5	72.23	687	0.78	0.08918 ± 0.9	2.2970 ± 4.1	0.1868 ± 4.0	0.05971 ± 4.5	474.8 ± 7.8	560.9 ± 98.2	927.6 ± 138.2	85	14.3	11.7	d
3	75.88	746	0.90	0.08656 ± 0.6	0.8935 ± 1.5	0.0749 ± 1.4	0.03053 ± 1.2	524.4 ± 3.0	521.6 ± 17.4	509.2 ± 16.9	101	2.1	5.13	524.4 7.8
6	78.79	796	0.59	0.08986 ± 0.8	1.0428 ± 2.7	0.0842 ± 2.6	0.03767 ± 2.8	537.5 ± 4.4	530.1 ± 23.3	498.4 ± 22.0	101	3.2	5.11	537.5 8.6
1	65.13	581	0.73	0.09771 ± 1.0	1.6355 ± 5.4	0.1214 ± 5.3	0.04836 ± 3.8	557.9 ± 7.6	559.6 ± 86.2	566.8 ± 86.7	100	7.5	4.56	557.9 10.8
10	36.68	392	0.35	0.09207 ± 0.5	0.7175 ± 1.6	0.0565 ± 1.5	0.02899 ± 1.3	567.2 ± 2.8	542.4 ± 8.3	439.4 ± 6.8	105	0.1	2.24	567.2 8.3
weighted mean of selected common-Pb corrected ages (n = 4 of 8, MSWD = 5.4, 1σ absolute external error)														545 16

Analytical methods described by Scott & Palin (2008) and references therein.
All errors are 1σ, * = radiogenic component only (common-Pb calculated using ^{208}Pb according to Compston et al. 1984), d = discordant, rd = reversely discordant. Spot-MSWD calculated on basis of scatter of observed data with increasing depth during individual spot measurement.

S.P. Lee dredge 17 were 73°40.8'S, 176°25.1'W, water depth 2250 m. A photograph of sample 17-3b-10 (Wong *et al.* 1987, fig. 7A) shows a subangular slab, *c.* 40 x 20 x 5 cm in size. A 5 x 5 x 3 cm trimmed piece of this rock was lodged in the New Zealand Geological Survey (later GNS Science) Petrology Collection at the time, and numbered P50869. From this sample we made a thin section, powder for whole rock analysis, and some mineral separates.

Wong *et al.* (1987, fig. 7B) described sample 17-3b-10 as a "meta rhyolite/tuff", an opinion with which we basically agree. Phenocrysts of quartz, oligoclase and microcline microperthite up to 1 mm in size are set in a microcrystalline matrix of quartz, feldspar, sericitic muscovite, titanite and biotite. The K-feldspar is turbid and consists of patchy intergrowths of simply twinned sanidine and cross-hatched microcline (Fig. 2b). One or two small pelitic xenoliths are present in the thin section. We cannot be sure if the original rock was a lava, tuff or shallow intrusion as there is a weak but distinct metamorphic foliation that anastomoses around the phenocrysts (technically porphyroclasts) and, of course, field relations are absent. The scattered fine-grained biotite in the matrix is clearly metamorphic but no other metamorphic index minerals are present. The fine grain size of the matrix and relict phenocrysts indicate to us that the porphyritic rhyolite probably underwent no more than greenschist facies recrystallization.

Petrochemical data

The chemical analysis (Table II) reveals the rock to be a subalkaline high-K rhyolite. Given the analysis of a small and metamorphosed sample, we are reluctant to interpret its geochemistry too much. The analysis is fairly typical for a rhyolite and, on the Y+Nb vs Rb granite tectonic discrimination diagram of Whalen *et al.* (1987) (not shown), plots very close to the mutual boundary of syncollisional, volcanic arc and within plate granites, i.e. the chemistry of this single sample is not especially distinctive. The chemistry is I-type to marginal A-type as it has low CaO/FeO* and Mg number, slightly high Ga/Al and rare earth elements and a large negative Eu anomaly. In these respects it is somewhat similar to two suites of siliceous igneous rocks in the Transantarctic Mountains: the 546 Ma Mulock Granite (Cottle & Cooper 2006), and rhyolite porphyries of the 516–525 Ma Liv Group (Wareham *et al.* 2001) (Fig. 1).

U-Pb zircon data

Due to the small available sample size, P50869 yielded very few zircon grains, most of which were themselves too small (< 30 μm wide) to analyse. Eight grains were analysed by LA-ICP-MS methods (Table III) and most of the analysed spots can be considered core or composite core-rim analyses (Fig. 4a). All grains plot as discordant on a Tera-Wasserburg plot (Fig. 4b). Discordance of the four oldest grains appears to be due to common Pb contamination and the three
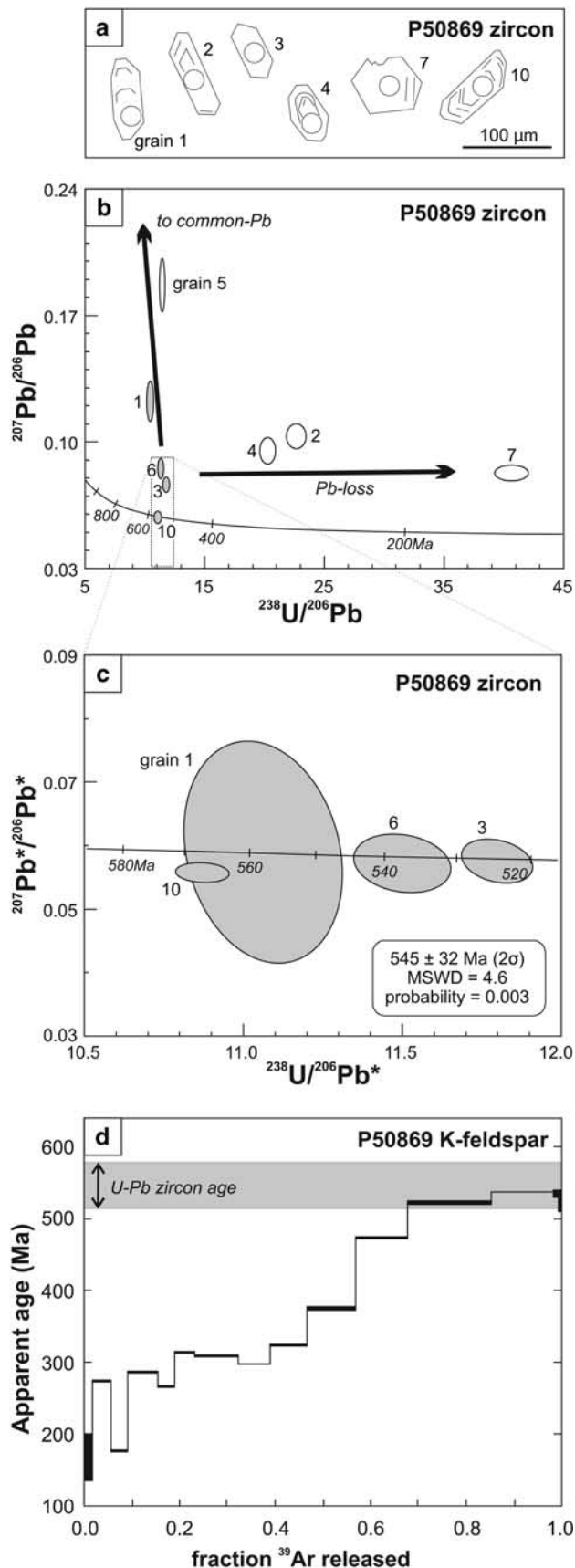
youngest grains scatter to lower $^{238}U/^{206}Pb$ ratios indicative of possible Pb loss. Correction of the analyses using the ^{208}Pb procedure of Compston *et al*. (1984) resulted in four analyses shifting to the concordia (Fig. 4c). The mean weighted age of these four zircons is 545 ± 32 Ma (2σ error) which we interpret as the age of crystallization of the rhyolite magma. We acknowledge that our pooled age for P50869 is based on few grains and is low precision, but believe it is adequate for the purposes of this study. The alternative hypothesis, that the Proterozoic–Cambrian zircons were inherited by a Mesozoic rhyolite, is less likely because: 1) the three youngest zircons have very high U concentrations and would have experienced lattice damage from a high time-integrated alpha dose, consistent with their observed major Pb loss and their higher spot MSWD values as compared to the five oldest zircons (Table III), 2) the observed xenoliths in P50869 are pelitic and would not have contributed 30–100 μm zircon grains to the rhyolite, and 3) the K-feldspar Ar-Ar data and the Sr and Nd isotope data also support a Proterozoic–Cambrian age (see below).

Ar-Ar K-feldspar data

The K-feldspar step heating results for P50869 are shown in Table IV and the argon release spectrum is plotted in Fig. 4d. Low temperature steps (about half the total gas) give ages from 270–300 Ma, after which the steps rise monotonically to a maximum of 540 Ma at high temperatures. No plateau is present and it is not possible to make a diffusion model of the spectrum to get a temperature-time history. The ages of the high temperature steps of the K-feldspar support the Precambrian–Cambrian age interpretation of the zircons. The lowering of argon age steps is consistent with the greenschist facies metamorphism of P50869. Greenschist facies metamorphic temperatures are sufficient to lower the ages of all except the most retentive domains of K-feldspars, and this age spectrum pattern is typical of argon loss induced by such thermal histories. Final closure to argon loss occurred in the Late Palaeozoic–Mesozoic, a feature also seen in Ar-Ar K-feldspar ages from plutonic rocks of southern Victoria Land (Calvert & Mortimer 2003).

Sr, Nd and Pb isotope data

The Precambrian–Cambrian age of the meta-rhyolite is further supported by Sr and Nd isotopic ratio calculations (Table II) which indicate time of closure of the isotopic systems. Using

Fig. 4. Geochronology of P50869. **a.** Line drawings of zoned zircon grains based on cathodoluminescence images (circles are analysed spots, no image for grains 5 or 6). **b.** Tera–Wasserburg plot of eight uncorrected U-Pb zircon analyses. **c.** Tera-Wasserburg plot of four common Pb corrected zircon analyses used for age determination. **d.** Ar-Ar step heating spectrum of K-feldspar; U-Pb zircon age of the sample is also shown.

Table IV. $^{40}Ar/^{39}Ar$ step heating data for K-feldspar from sample P50869 Iselin Bank meta-rhyolite.

Temp (°C)	Time (min)	$^{40}Ar/^{39}Ar$	$^{36}Ar/^{39}Ar$ x 100	$^{37}Ar/^{39}Ar$ x 1000	^{39}Ar (E^{-14} mol)	Ca/K	% cum. ^{39}Ar	% $^{40}Ar*$	$^{40}Ar*/^{39}Ar_K$	Calculated age (Ma) ± 1σ
450	15	427.0	24.25	8.639	0.168	0.0164	0.1	83.2	355.3	1669.0 ± 5.3
450	35	114.1	18.30	32.82	0.170	0.0624	0.2	52.6	60.09	413.3 ± 6.8
550	15	213.7	8.090	8.862	1.257	0.0168	0.8	88.8	189.9	1074.0 ± 4.7
550	35	23.81	1.899	15.85	1.575	0.0301	1.7	76.3	18.17	135.3 ± 0.7
650	15	40.24	0.6898	38.19	7.828	0.0726	5.8	94.9	38.18	273.3 ± 0.8
650	35	24.47	0.2003	69.51	6.566	0.1320	9.2	97.5	23.87	175.6 ± 0.7
750	15	40.98	0.2528	84.52	11.89	0.1610	15.4	98.1	40.21	286.8 ± 1.2
750	35	37.81	0.2053	17.89	6.503	0.0340	18.8	98.3	37.19	266.7 ± 0.9
850	15	45.79	0.4744	8.726	8.124	0.0166	23.1	96.9	44.36	313.9 ± 1.2
950	15	44.24	0.2364	7.402	17.82	0.0141	32.4	98.4	43.52	308.4 ± 1.0
1000	15	43.00	0.3823	5.996	12.49	0.0114	38.9	97.3	41.83	297.4 ± 0.9
1050	15	47.09	0.4581	11.54	14.55	0.0219	46.5	97.1	45.72	322.7 ± 1.4
1100	15	55.23	0.4279	11.40	19.70	0.0217	56.8	97.7	53.92	375.0 ± 1.5
1150	15	71.46	0.4560	12.84	21.13	0.0244	67.8	98.1	70.08	473.7 ± 1.7
1190	15	79.00	0.2007	2.366	33.19	0.0045	85.2	99.2	78.38	522.4 ± 2.3
1220	15	81.85	0.2749	0.063	25.18	0.0001	98.4	99.0	81.03	537.6 ± 1.1
1250	15	89.93	3.172	0.000	1.996	0.0000	99.4	89.5	80.54	534.8 ± 5.8
1300	15	106.7	9.469	8.362	0.981	0.0159	99.9	73.8	78.78	524.7 ± 14
1370	15	414.1	118.5	128.5	0.119	0.2440	99.9	15.4	63.86	436.3 ± 188
1450	30	10985	3699	2241	0.008	4.2700	100.0	0.5	54.16	376.4 ± 62632
								Total	58.91	406.0 ± 4.1

Methods follow McLaren *et al.* 2002. Sample weight 23.30 mg, Irradiation ANU 119, J = 0.0042844 ± 0.4%. Data corrected for mass spectrometer discrimination, line blanks, and for the decay of ^{37}Ar and ^{39}Ar during and after irradiation. $^{40}Ar*$ is radiogenic ^{40}Ar, and $^{39}Ar_K$ is potassium-derived ^{39}Ar. Corrections for interfering isotopes have only been applied to $^{40}Ar*/^{39}Ar_K$. Amounts of ^{39}Ar are derived from the measured sensitivity of the mass spectrometer. Relative isotope amounts are precise, but absolute amounts may have uncertainties of *c.* 10%. Totals are the %^{39}Ar weighted means of the analyses. Flux monitor: Australian National University GA1550 Biotite (98.5 Ma, J determined by interpolation). l = 5.543×10^{-10} a^{-1}. Correction factors were derived from analysis of CaF$_2$ and synthetic K-glass: $^{(40/39)}$K = 0.027, $^{(36/37)}$Ca = 0.00035, $^{(39/37)}$Ca = 0.000786.

a model age of 513 Ma (the lower 2σ limit of the zircon age) gives $^{87}Sr/^{86}Sr_i = 0.7055$ and $\varepsilon Nd_i = -8.2$. Although these values appear decoupled (Sr is far less radiogenic than Nd on typical crustal arrays (not shown), possibly because of sensitivity to Rb/Sr ratio, e.g. by alteration or small sample size bias) they are not unreasonable for Precambrian–Cambrian Ross Orogen siliceous igneous rocks (Cox *et al.* 2000, Wareham *et al.* 2001). In contrast, a model age of 100 Ma gives unreasonably high radiogenic isotopic ratios of $^{87}Sr/^{86}Sr = 0.7744$ and $\varepsilon Nd_i = -11.8$ for siliceous igneous rocks that have I- and A-type characteristics. The Pb isotope ratios of P50869 resemble those reported for the DV1b suite of Cox *et al.* (2000) from the Transantarctic Mountains.

Discussion

DSDP 270 correlation

The closest onland occurrence of calcsilicate gneisses and marble to DSDP 270 is in the Skelton Group of southern Victoria Land and this is what influenced Ford & Barrett (1975) to correlate the DSDP 270 basement with the Ross Orogen. However, it is problematic that carbonates and calcsilicates are so rare in all the peri-Ross Sea orogenic belts and yet this rock type constitutes all ten metres of sampled DSDP 270 basement. We agree, that on the basis of abundance of marble and calcsilicate, and in the absence

of any geochronological data, a Ross Orogen correlation was probably the best choice. However, calcareous rocks do occur within the Bowers Terrane (Bradshaw *et al.* 1985 and references therein) and scattered calcsilicate nodules, sometimes with quartz–calcite–pyroxene–garnet assemblages have been reported from the Swanson Formation and from the Lachlan Orogen (Bradshaw *et al.* 1983, Adams 1986, Morand 1994). Rare marbles have also been reported from Robertson Bay Group and Swanson Formation (Wade & Couch 1982), and scattered, rare limestones are present in the Lachlan Orogen. Because calcareous rocks are present in small amounts in both the orogenic belts under consideration, the age and grade of metamorphism becomes relevant when making a correlation.

Based on a (representative but non-exhaustive) compilation of metamorphic ages from the relevant orogens (Fig. 5), the 437 ± 6 Ma age of amphibolite facies metamorphism seems too young to be typical Ross Orogen as the youngest argon ages (which represent cooling in the greenschist facies) in the Ross Orogen are 460 Ma or older. In contrast, deformation was continuing and/or active in the Silurian in the more Pacific-ward Lachlan–Tuhua–Robertson Bay–Swanson Orogen and in the Bowers Terrane between the two orogens (Adams 2006). On this basis, we provisionally interpret the DSDP 270 metamorphic basement as probable Lachlan–Tuhua–Robertson Bay–Swanson Orogen, with an even more speculative correlation to the Bowers Terrane.
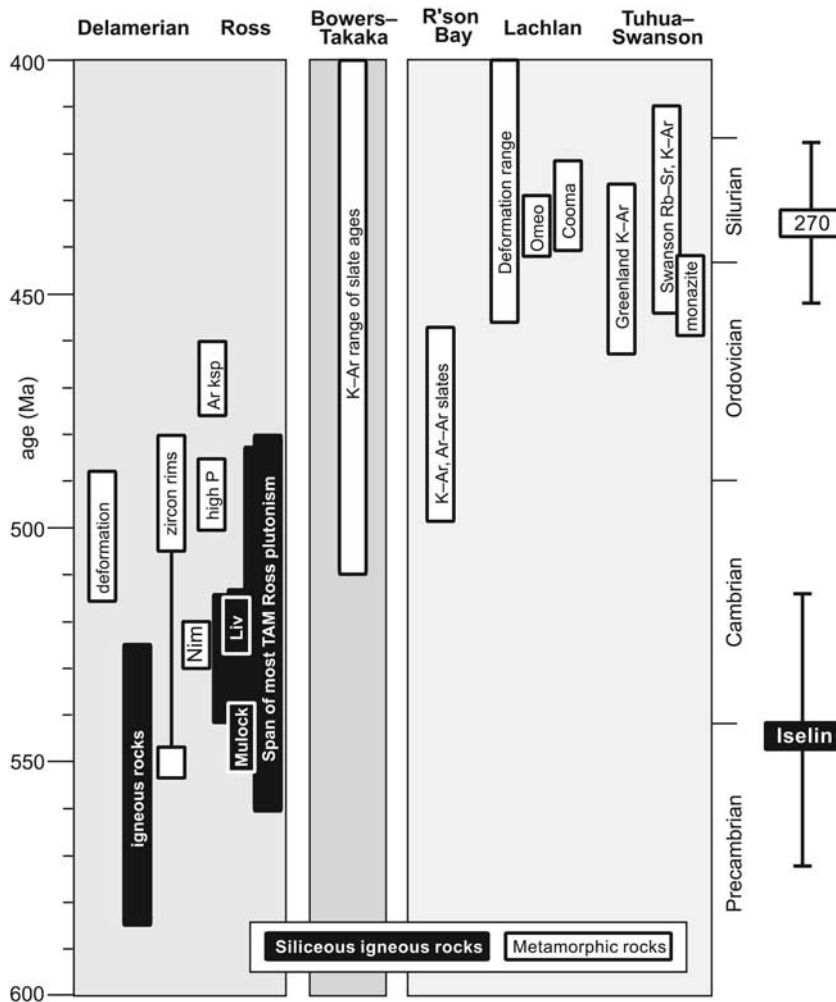
Fig. 5. Time space plot comparing new geochronological data from DSDP 270 and Iselin Bank with other data from the Ross–Delamerian, and Lachlan–Robertson Bay–Swanson orogens. Reference data from Morand (1990), Dallmeyer & Wright (1992), Ghiribelli *et al.* (2002), Goodge (2002), Calvert & Mortimer (2003), Wysoczanski & Allibone (2004), Adams (2004, 2006), Glen (2005) and Cooper *et al.* (2010).

Iselin Bank correlation

Although the 545 ± 32 Ma age for the Iselin Bank meta-rhyolite is not especially precise, the U-Pb, Ar-Ar and tracer isotope data are all consistent with a latest Neoproterozoic to earliest Cambrian eruptive/intrusive age. Most siliceous igneous rocks of this age around the Ross Sea area are plutonic (e.g. Granite Harbour Intrusives and constituent suites) (Stump 1995, Allibone & Wysoczanski 2002), although eruptive equivalents such as the Liv Group are also known (Stump 1995, Wareham *et al.* 2001). The Ross Orogen appears to be the only feasible Antarctic source as Late Proterozoic–Cambrian siliceous igneous rocks are unknown from Bowers Terrane and/or the Lachlan–Tuhua–Robertson Bay–Swanson Orogen (Fig. 5).

The complex zircon systematics (variable inheritance and variable Pb loss) of P50869 are typical of 500–550 Ma pre- and syn-kinematic Ross granitoids (e.g. Cox *et al.* 2000, Allibone & Wysoczanski 2002, Cottle & Cooper 2006). Ross zircons contrast with those from the Admiralty Intrusives that intrude Robertson Bay Terrane and the Ford

Granodiorite that intrudes Swanson Formation, both of which are Devonian–Carboniferous (340–380 Ma) and have well-clustered zircon spectra with very little inheritance or Pb loss (Pankhurst *et al.* 1998).

We interpret the Iselin Bank meta-rhyolite P50869 to correlate with similar igneous rocks in the Ross Orogen. As previously mentioned, Wong *et al.* (1987) regarded the meta-rhyolite as the only dredge sample from the Iselin Bank that could have been *in situ*. A till provenance study by Licht *et al.* (2005) showed ice stream directions from the southern Transantarctic Mountains towards the Iselin Bank during the last glacial maximum. We acknowledge the possibility remains open that P50869 could have been glacially transported. The remaining discussion in this paper assumes that the Iselin Bank meta-rhyolite is *in situ*.

Definition and extent of the Ross-Delamerian Orogen

Bradshaw (2007) noted that many papers treat the Robertson Bay Terrane (RBT) of northern Victoria Land as part of the Ross Orogen, but that: 1) the RBT lacks a demonstrable

Early Cambrian deformation, and 2) the Ordovician–Silurian penetrative deformation of the RBT cannot be shown to extend into the Wilson Terrane. Figure 1 follows Bradshaw (2007) in defining three major orogenic belts in the Transantarctic Mountains–Ross Sea–Marie Byrd Land area. In this context, Bradshaw (2007) drew attention to a few outliers of Ross Orogen (or older) rocks that were outside the generally recognized Ross–Delamerian Orogen (Fig. 1): a 512 Ma granite at Surgeon Island, a 505 Ma orthogneiss at Mount Murphy, > 1100 Ma peridotite xenoliths from the Executive Committee Range, and calcsilicate gneiss at DSDP 270. To this can be added some 480–510 Ma orthogneisses in Fiordland, New Zealand (Gibson & Ireland 1996, Allibone *et al.* 2010). As shown above, we do not now regard the DSDP 270 rocks as being part of the Ross Orogen. However, assuming it is *in situ*, the Iselin Bank meta-rhyolite may be another example of an occurrence of Ross Orogen rocks outside the main linear belt of the Ross–Delamerian Orogen.

In addition, possible Bowers Terrane equivalents on Campbell Island, a 1119 Ma Grenville Orogen syenite dredged from the western South Tasman Rise and a 1167 Ma granite dredged from the edge of the Campbell Plateau (Challis *et al.* 1982, Fioretti *et al.* 2005a, Adams 2007; Fig. 1) may also be tectonically allochthonous pieces of older orogens but, as with the Iselin Bank, it is far from certain that the two dredged samples are *in situ*. On the basis of Hf isotope studies of zircons, Flowerdew *et al.* (2006) inferred the presence of late Mesoproterozoic crust underneath parts of the Antarctic Peninsula. The size, mechanism and timing of dispersal of pieces of Precambrian–Cambrian crust into younger parts of Cawood's (2005) Terra Australis Orogen, remains speculative. Options include Ordovician rifting (Bradshaw 2007), strike-slip faulting oblique to the orogen, and/or orogen-subperpendicular low-angle extensional exhumation of Ross basement.

Conclusions

Titanite from a calcsilicate gneiss in DSDP 270 gives an early Silurian U-Pb age, that we interpret to be the age of amphibolite facies metamorphism. This age is too young for typical Ross Orogen high-grade metamorphism and we suggest a correlation with the Lachlan–Tuhua–Robertson Bay–Swanson Orogen, possibly the Bowers Terrane.

A meta-rhyolite from the Iselin Bank, Ross Sea, Antarctica, is of latest Neoproterozoic to earliest Cambrian age. We correlate it with rocks of similar age and composition in the Ross–Delamerian Orogen of the Transantarctic Mountains. If the material is not ice-rafted debris, then the Iselin Bank sample represents an additional occurrence of Ross Orogen basement found outside the main Transantarctic Mountains.

Acknowledgements

References

ADAMS, C.J. 1986. Geochronological studies of the Swanson Formation of Marie Byrd Land, West Antarctica, and correlation with northern Victoria Land, East Antarctica and the South Island, New Zealand. *New Zealand Journal of Geology and Geophysics*, **29**, 345–358.

ADAMS, C.J. 2004. Rb-Sr age and strontium isotope characteristics of the Greenland Group, Buller Terrane, New Zealand, and correlations at the East Gondwanaland margin. *New Zealand Journal of Geology and Geophysics*, **47**, 189–200.

ADAMS, C.J. 2006. Styles of uplift of Paleozoic terranes in northern Victoria Land, Antarctica: evidence from K–Ar patterns. *In* FÜTTERER, D.K., DANASKE, D., KLEINSCHMIDT, G., MILLER, H. & TESSENSOHN, F., eds. *Antarctica: contributions to global earth sciences*. Heidelberg: Springer, 205–214.

ADAMS, C.J. 2007. Geochronology of Paleozoic terranes at the Pacific Ocean margin of Zealandia. *Gondwana Research*, **13**, 250–258.

ALLIBONE, A.H. & WYSOCZANSKI, R.J. 2002. Initiation of magmatism during the Cambro–Ordovician Ross orogeny in southern Victoria Land, Antarctica. *Geological Society America Bulletin*, **114**, 1007–1018.

ALLIBONE, A.H., JONGENS, R., TURNBULL, I.M., MILAN, L.A., DACZKO, N.R., DE PAOLI, M.C. & TULLOCH, A.J. 2010. Plutonic rocks of western Fiordland, New Zealand: field relations, geochemistry, correlation, and nomenclature. *New Zealand Journal of Geology and Geophysics*, **52**, 379–415.

BRADSHAW, J.D. 2007. The Ross Orogen and Lachlan Fold Belt in Marie Byrd Land, northern Victoria Land and New Zealand: implication for the tectonic setting of the Lachlan Fold Belt in Antarctica. *In* COOPER, A.K., RAYMOND, C.R., et al. eds. *Antarctica: a keystone in a changing world - Online Proceedings of the 10th ISAES*. USGS Open-File Report 2007-1047, Short Research Paper 059.

BRADSHAW, J.D., ANDREWS, P.B. & FIELD, B.D. 1983. Swanson Formation and related rocks of Marie Byrd Land and comparison with the Robertson Bay Group of north Victoria Land. *In* OLIVER, R.L., JAMES, P.R. & JAGO, J.B., eds. *Antarctic earth science*. Canberra: Australian Academy of Science, 274–279.

BRADSHAW, J.D., WEAVER, S.D. & LAIRD, M.G. 1985. Suspect terranes and Cambrian tectonics in northern Victoria land, Antarctica. *In* HOWELL, D.G., ed. *Tectonostratigraphic terranes of the circum-Pacific region*. Circum-Pacific Council for Energy and Mineral Resources, Houston, Earth Science Series, **1**, 467–479.

BRADSHAW, J.D., GUTJAHR, M., WEAVER, S.D. & BASSETT, K.N. 2009. Cambrian intra-oceanic arc accretion to the austral Gondwana margin: constraints on the location of proto-New Zealand. *Australian Journal of Earth Sciences*, **56**, 587–594.

CALVERT, A.T. & MORTIMER, N. 2003. Thermal history of Transantarctic Mountains K-feldspars, southern Victoria Land. *Terra Antartica*, **10**, 3–15.

CAWOOD, P.A. 2005. Terra Australis Orogen: Rodinia breakup and development of the Pacific and Iapetus margins of Gondwana during the Neoproterozoic and Paleozoic. *Earth Science Reviews*, **69**, 249–279.

CHALLIS, G.A., GABITES, J. & DAVEY, F.J. 1982. Precambrian granite and manganese nodules dredged from southwestern Campbell Plateau, New Zealand. *New Zealand Journal of Geology and Geophysics*, **25**, 493–497.

COMPSTON, W., WILLIAMS, I.S. & MEYER, C. 1984. U-Pb geochronology of zircons from lunar Breccia 73217 using a sensitive high mass-resolution ion microprobe. *Journal of Geophysical Research*, **89**, 525–534.

COOK, Y. & CRAW, D. 2002. Neoproterozoic structural slices in the Ross Orogen, Skelton Glacier area, South Victoria Land, Antarctica. *New Zealand Journal of Geology and Geophysics*, **45**, 133–143.

COOPER, A.F., MAAS, R., SCOTT, J.M. & BARBER, A.J.W. 2010. Dating of volcanism and sedimentation in the Skelton Group, Transantarctic Mountains: implications for the Rodinia-Gondwana transition in southern Victoria Land, Antarctica. *Geological Society of America Bulletin*, 10.1130/B30237.1

COTTLE, J.M. & COOPER, A.F. 2006. Geology, geochemistry, and geochronology of an A-type granite in the Mulock Glacier area, southern Victoria Land, Antarctica. *New Zealand Journal of Geology and Geophysics*, **49**, 191–202.

COX, S.C., PARKINSON, D.L., ALLIBONE, A.H. & COOPER, A.F. 2000. Isotopic character of Cambro-Ordovician plutonism, southern Victoria Land, Antarctica. *New Zealand Journal of Geology and Geophysics*, **43**, 501–520.

DALLMEYER, R.D. & WRIGHT, T.O. 1992. Diachronous cleavage development in the Robertson Bay Terrane, Northern Victoria Land, Antarctica: tectonic implications. *Tectonics*, **11**, 437–448.

FIORETTI, A.M., BLACK, L.P., FODEN, J. & VISONA, D. 2005a. Grenville-age magmatism at the South Tasman Rise (Australia): a new piercing point for the reconstruction of Rodinia. *Geology*, **33**, 769–772.

FIORETTI, A.M., CAPPONI, G., BLACK, L.P., VARNE, R. & VISONA, D. 2005b. Surgeon Island granite SHRIMP zircon ages: a clue for the Cambrian tectonic setting and evolution of the Paleopacific margin of Gondwana (northern Victoria Land, Antarctica). *Terra Nova*, **17**, 242–249.

FITZGERALD, P.G. & BALDWIN, S. 1997. Detachment fault model for evolution of the Ross Embayment. *In* RICCI, C.A., *ed. The Antarctic region: processes and evolution*. Siena: Terra Antartica Publications, 555–564.

FLOWERDEW, M.J., MILLAR, I.L., VAUGHAN, A.P.M., HORSTWOOD, M.S.A. & FANNING, C.M. 2006. The source of granitic gneisses and migmatites in the Antarctic Peninsula: a combined U-Pb SHRIMP and laser ablation Hf isotope study of complex zircons. *Contributions to Mineralogy and Petrology*, **151**, 751–768.

FORD, A.B. & BARRETT, P.J. 1975. Basement rocks of the south-central Ross Sea, Site 270. *In* HAYES, D.E., *ed. Initial Reports, Deep Sea Drilling Project 28*. Washington, DC: US Government Printing Office, 861–868.

GARBE-SCHÖNBERG, C.D. 1993. Simultaneous determination of thirty-seven trace elements in twenty eight rocks standards by ICP-MS. *Geostandards Newsletter*, **17**, 151–178.

GHIRIBELLI, B., FREZZOTTI, M.L. & PALMERI, R. 2002. Coesite in eclogites of the Lanterman Range (Antarctica): evidence form textural and Raman studies. *European Journal of Mineralogy*, **14**, 355–360.

GIBSON, G.M. & IRELAND, T.R. 1996. Extension of Delamerian (Ross) orogen into western New Zealand: evidence from zircon ages and implications for crustal growth along the Pacific margin of Gondwana. *Geology*, **24**, 1087–1090.

GLEN, R.A. 2005. The Tasmanides of eastern Australia. *In* VAUGHAN, A.P.M., LEAT, P.L. & PANKHURST, R.J., *eds. Terrane processes at the margins of Gondwana. Geological Society, London, Special Publication*, **246**, 23–96.

GOODGE, J.W. 2002. From Rodinia to Gondwana: supercontinent evolution in the Transantarctic Mountains. *In* GAMBLE, J. & SKINNER, D.N.B., *eds. Proceedings of the 8th International Symposium on Antarctic Earth Science. Royal Society of New Zealand Bulletin*, **35**, 61–74.

HOERNLE, K., HAUFF, F. & VAN DEN BOGAARD, P. 2004. 70 m.y. history (139–69 Ma) for the Caribbean large igneous province. *Geology*, **32**, 697–700.

KENNEDY, P.C., ROSER, B.P. & HUNT, J.L. 1983. Analyses of the USGS geochemical reference samples GXR-1 to 6. *Geostandards Newsletter*, **7**.

LAIRD, M.G. 1991. The Late Proterozoic-Middle Palaeozoic rocks of Antarctica. *In* TINGEY, R.J., *ed. The geology of Antarctica*. Oxford: Oxford University Press, 74–119.

LICHT, K.J., LEDERER, J.R. & SWOPE, J.R. 2005. Provenance of LGM glacial till (sand fraction) across the Ross Embayment, Antarctica. *Quaternary Science Reviews*, **24**, 1499–1520.

MCLAREN, S.M., DUNLAP, W.J., SANDIFORD, M. & MCDOUGALL, I. 2002. Thermochronology of high heat-producing crust at Mount Painter, South Australia: implications for tectonic reactivation of continental interiors. *Tectonics*, **21**, 1–18.

MORAND, V.J. 1990. Low-pressure regional metamorphism in the Omeo Metamorphic Complex, Victoria, Australia. *Journal of Metamorphic Geology*, **8**, 1–12.

MORAND, V.J. 1994. Geological note: calc-silicate lenses in the early Palaeozoic mud-pile of the Lachlan fold belt. *Australian Journal of Earth Sciences*, **41**, 383–386.

PANKHURST, R.J., WEAVER, S.D., BRADSHAW, J.D., STOREY, B.C. & IRELAND, T.R. 1998. Geochronology and geochemistry of pre-Jurassic superterranes in Marie Byrd Land, Antarctica. *Journal Geophysical Research*, **103**, 2529–2547.

SCOTT, J.M. & PALIN, J.M. 2008. LA-ICP-MS U-Pb zircon ages from Mesozoic plutonic rocks in eastern Fiordland, New Zealand. *New Zealand Journal Geology and Geophysics*, **51**, 105–113.

SCOTT, J.M., COOPER, A.F., PALIN, J.M., TULLOCH, A.J., KULA, J., JONGENS, R.J., SPELL, T.L. & PEARSON, N.J. 2009. Tracking the influence of a continental margin on growth of a magmatic arc, Fiordland, New Zealand, using thermobarometry, thermochronology, and zircon U-Pb and Hf isotopes. *Tectonics*, **28**, 10.1029/2009TC002489.

STUMP, E. 1995. *The Ross Orogen of the Transantarctic Mountains*. Cambridge: Cambridge University Press, 284 pp.

WADE, F.A. & COUCH, D.R. 1982. The Swanson Formation, Ford Ranges, Marie Byrd Land - evidence for and against a direct relationship with the Robertson Bay group, northern Victoria Land. *In* CRADDOCK, C., *ed. Antarctic geoscience*. Madison, WI: University of Wisconsin Press, 609–616.

WAREHAM, C.D., STUMP, E., STOREY, B.C., MILLAR, I.L. & RILEY, T.R. 2001. Petrogenesis of the Cambrian Liv Group, a bimodal volcanic rock suite from the Ross orogen, Transantarctic Mountains. *Geological Society of America Bulletin*, **113**, 360–372.

WHALEN, J.B., CURRIE, K.L. & CHAPPELL, B.W. 1987. A-type granites: geochemical characteristics, discrimination and petrogenesis. *Contributions to Mineralogy and Petrology*, **95**, 407–419.

WONG, F.L., BARRETT, P.J., GAMBLE, J.A. & HOWELL, D.G. 1987. Petrography of rock samples dredged from the Iselin Bank, Ross Sea, Antarctica. *In* COOPER, A.K. & DAVEY, F.J., *eds. The Antarctic continental margin: geology and geophysics of the western Ross Sea*. Houston, TX: Circum-Pacific Council for Energy and Mineral Resources, 231–253.

WYSOCZANSKI, R.J. & ALLIBONE, A.H. 2004. Age, correlation, and provenance of the Neoproterozoic Skelton Group, Antarctica: Grenville age detritus on the margin of East Antarctica. *Journal of Geology*, **112**, 401–416.